Anisotropic Heisenberg model with dipolar interactions: Monte Carlo simulations of the planar-to-paramagnetic phase transition in a bilayer system

L. A. S. Mól* and B. V. Costa†

Departamento de Física, Laboratório de Simulação, ICEX, UFMG, Caixa Postal 702, 31270-901 Belo Horizonte, MG, Brazil

(Received 7 October 2008; revised manuscript received 28 November 2008; published 3 February 2009)

In this work we used extensive Monte Carlo simulations and finite-size scaling theory to study the planar-to-paramagnetic phase transition in the dipolar-anisotropic Heisenberg model in a bilayer system. This model is a prototype to describe ferromagnetic thin films. Our results suggest that this is an order-disorder phase transition that might belong to another universality class characterized by a nondivergent specific heat ($\alpha \approx -0.4$) and the critical exponents $\nu=1.22(9)$, $\gamma=2.1(2)$, and $\beta=0.18(5)$.

DOI: 10.1103/PhysRevB.79.054404 PACS number(s): 75.40.Cx

I. INTRODUCTION

Dipolar interactions play an essential role in the magnetic properties of low-dimensional systems. For example, it was experimentally observed that in magnetic nanodisks dipolar interactions induce the formation of a vortex in the system.[1–3] In ferromagnetic ultrathin films the interplay between dipolar interactions and magnetocrystalline anisotropies is responsible for a reorientation transition.[4,5] In this kind of transition the spins are aligned out-of-plane at low temperatures and as the temperature increases a reorientation to an in-plane configuration is observed. Besides that, the existence of ferromagnetic order in two-dimensional systems is a consequence of the presence of anisotropies and/or long-range interactions. Mermin and Wagner[6] in a seminal paper showed that isotropic ferromagnets with short-range interactions do not present long-range order at any finite temperature in two dimensions. The absence of long-range order in such systems does not imply the absence of a phase transition. It is well known that in the *XY* model in two dimensions there is a phase transition from a phase with algebraic decaying correlations to a phase with exponentially decaying correlations. The most accepted phenomenology to explain this phase transition is the unbinding of vortex-antivortex pairs.[7,8] This is the Berezinskii-Kosterlitz-Thouless (BKT) phase transition. In a real magnet, dipolar interactions between magnetic moments are always present. The presence of such interaction is sufficient to stabilize the magnetization as shown by Maleev.[9] In addition, the presence of interfaces induces the appearance of anisotropies which can also give rise to long-range order. The existence of long-range order in a system with both interactions was analyzed by Bruno.[10]

The main features of ferromagnetic ultrathin films of interest to us in this paper is recovered by a model including three different interactions, namely, exchange interactions, single-ion easy-axis anisotropy, and dipolar interactions which can be summarized in the following prototype Hamiltonian:

$$H = -J\sum_{\langle i,j\rangle} \vec{S}_i \cdot \vec{S}_j - A\sum_i (S_i^z)^2 + D\sum_{i\neq j}\left[\frac{\vec{S}_i\cdot\vec{S}_j}{r_{ij}^3} - \frac{3(\vec{S}_i\cdot\vec{r}_{ij})(\vec{S}_j\cdot\vec{r}_{ij})}{r_{ij}^5}\right]. \quad (1)$$

Here, $J>0$ defines a ferromagnetic exchange constant, $A>0$ is an easy-axis anisotropy, and D is the dipolar constant. $\vec{S}_i=(S_i^x,S_i^y,S_i^z)$ is a classical spin variable at the site i with $|\vec{S}_i|=1$ and $\vec{r}_{ij}$ connects sites i and j. $\langle i,j\rangle$ means that the first summation is to be evaluated only for nearest neighbors, the summation in the second term is over the whole lattice sites, and for the dipolar interaction the summation is evaluated over all pairs $i\neq j$. The dipolar-anisotropic Heisenberg (*d-AH*) model [Eq. (1)] has been studied in connection with the reorientation transition and the stripe and tetragonal phases.[11–17] Its phase diagram was first obtained numerically by Santamaria and Diep[12] for $J=1$, $A=2$, and $0.12<D<0.17$. They studied the model in a square lattice using a cutoff $r_0=6$ in the dipolar interaction. Rapini *et al.*,[14] using the same approach studied the model for $J=A=1$ and $0.1\leq D\leq 0.2$. In Fig. 1 we show a sketch of the phase diagram based in their works. The line labeled *a* is an Ising-type, Z_2, transition between an ordered ferromagnetic easy-axis phase and a paramagnetic phase. Line *b* is a first-order transition between the easy-axis and planar phases while the *c* line was found to be a BKT transition.[14] The found BKT transition seems to be a consequence of the cutoff introduced in the evaluation of dipolar interactions since when full long-range dipolar interactions are considered, the system exhibits long-range order.[9,10] Another attempt to determine the character of the planar-to-paramagnetic phase transition was done by Maier and Schwabl.[18] In their work, the authors considered

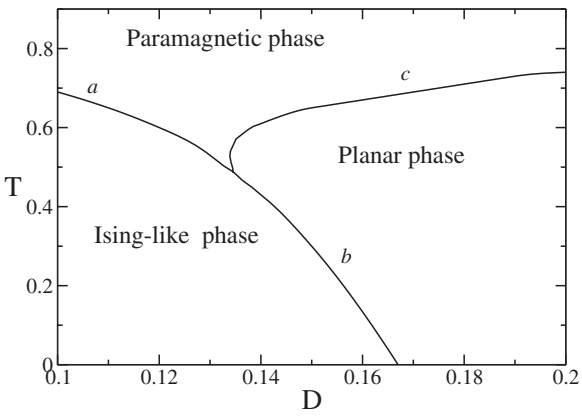

FIG. 1. Phase diagram of Hamiltonian (1) for $J=A=1$ based on the work of Santamaria and Diep (Ref. 12) and of Rapini *et al.* (Ref. 14).

the *XY* model (two spin components) with dipolar interactions. Their results should describe the d-AH model in the limit of small anisotropy when spins are expected to lie in plane. Using renormalization group techniques, they discussed the existence of a new universality class with characteristics of BKT and order-disorder transitions as well. They argued that the dipolar *XY* model exhibit long-range order at low temperature, but the correlation length diverges exponentially as the critical temperature is approached. The specific heat does not present any divergence as in a BKT transition. The susceptibility was expected to diverge as $\chi \propto \xi^{-\tilde{\gamma}}$, where $\tilde{\gamma}=\gamma/\nu=1$ is the critical susceptibility exponent and ξ is the correlation length. The magnetization approaches zero as $M \propto \xi^{-\tilde{\beta}}$, where $\tilde{\beta}=\beta/\nu=1/2$, and the correlation function exponent was found to be $\tilde{\eta}=\eta/\nu=1$. In this way, some questions regarding the planar-to-paramagnetic phase transition arise: (i) Is there a cutoff value where the phase transition changes from BKT to that found by Maier? (ii) Does the inclusion of a second layer in the system work as an anisotropy making the transition found by Rapini *et al.* more evident? We mean, is this transition a BKT type, as found by those authors, or is it in another universality class? Our aim in this paper is to answer question (ii). To this end we have performed extensive Monte Carlo simulations to study the model Hamiltonian [Eq. (1)] in a simple cubic lattice with two layers. The outline of the paper is as follows. Section II contains a description of our Monte Carlo procedure and finite-size scaling functions. In Sec. III, we present our numerical results and the analysis of some critical exponents. Finally, Sec. IV is devoted to the discussion of the results and conclusions.

II. MONTE CARLO METHOD AND FINITE-SIZE SCALING THEORY

Our system consists of simple cubic lattices with dimensions $L \times L \times 2$. In our notation the direction perpendicular to the film plane corresponds to the z axis. At each site of the lattice we defined a classical spin variable $\vec{S}_i=(S_i^x,S_i^y,S_i^z)$. The interactions are defined by Eq. (1). In the evaluation of dipolar interactions a cutoff was introduced at $r_0=5a$, where a is the lattice spacing, i.e., we have assumed that for $r_{ij}>5a$ the contribution of the dipolar part for the Hamiltonian is zero. Periodic boundary conditions were applied in the x and y directions, while in z open boundary conditions were used. In all simulations we assumed $J=A=1$ and $D=0.3$, so that we deal with the planar-to-paramagnetic phase transition (see Figs. 1 and 2). In this work the energy is measured in units of JS^2 and the temperature is in units of JS^2/k_B.

Our Monte Carlo scheme was a plain METROPOLIS algorithm[19,20] since conventional cluster algorithms cannot be used due to the long-range anisotropic character of the dipolar interactions. We define a Monte Carlo step (MCS) as consisting of an attempt to assign a new random direction to each spin in the lattice. To equilibrate the system it was used $100 \times L^2$ MCS which was found to be sufficient to reach equilibrium even in the vicinity of the phase transition. We have performed two sets of simulations. In the first set we

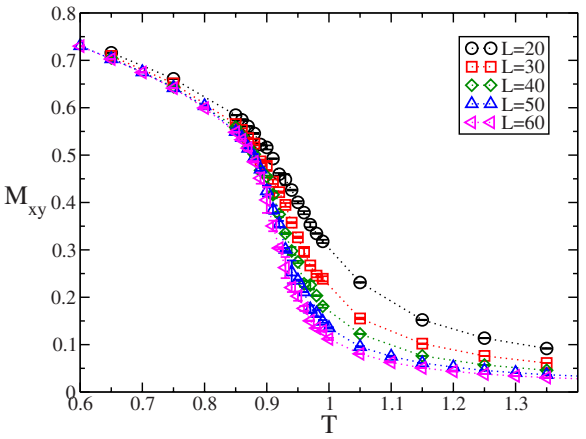

FIG. 2. (Color online) Planar magnetization as a function of temperature for $20<L<60$.

preliminarily explore the thermodynamic behavior of the model. A conventional Monte Carlo calculation is done in order to determine the position of the maxima of the specific heat and susceptibilities and the crossings of the fourth-order Binder's cumulant. We used in this first approach lattice sizes in the interval $20 \leq L \leq 60$. Once the possible transition temperature is determined, we refine the results by using the histogram method.[21,22] We produce the histograms for each lattice size in the interval $20 \leq L \leq 120$. The histograms are built at/close to the temperatures corresponding to the maxima obtained in the first step. With the single-histogram technique it is possible to estimate thermodynamic quantities of interest in a narrow temperature range around the simulated temperature. This technique is very useful to precisely locate the extrema of response functions. Nevertheless, when larger temperature ranges are required, the simple histogram method fails. To improve our results we constructed multiple histograms close to the transition temperature.[22] The multiple-histogram technique gives us one tool to improve the estimates of the thermodynamic quantities in a larger temperature range by combining histograms from simulations carried out at several slightly different temperatures. Details of these methods can be found in Refs. 21 and 22. The thermodynamic quantities on which we concentrated our attention were the specific heat, planar magnetization, planar susceptibility, fourth-order Binder's cumulant, and moments of magnetization as described below. The specific heat is defined as

$$c_v = \frac{\langle E^2 \rangle - \langle E \rangle^2}{N k_B T^2}, \tag{2}$$

where E is the internal energy of the system [computed using Eq. (1)] and $N=2 \times L^2$ is the lattice volume. The planar magnetization is

$$M_{xy} = \frac{1}{N}\langle m \rangle, \tag{3}$$

where

$$m = \sqrt{\left(\sum_{i=1}^{N} S_i^x\right)^2 + \left(\sum_{i=1}^{N} S_i^y\right)^2}.$$

The planar susceptibility is defined by the planar magnetization fluctuations as

$$\chi_{xy} = \frac{\langle m^2\rangle - \langle m\rangle^2}{Nk_BT}. \tag{4}$$

The fourth-order Binder's cumulant reads

$$U_4 = 1 - \frac{\langle m^4\rangle}{3\langle m^2\rangle^2}. \tag{5}$$

In order to calculate the critical exponent ν, we also defined the following moments of the planar magnetization:[23]

$$V_1 \equiv 4[m^3] - 3[m^4], \tag{6a}$$

$$V_2 \equiv 2[m^2] - [m^4], \tag{6b}$$

$$V_3 \equiv 3[m^2] - 2[m^3], \tag{6c}$$

$$V_4 \equiv \{4[m] - [m^4]\}/3, \tag{6d}$$

$$V_5 \equiv \{3[m] - [m^3]\}/2, \tag{6e}$$

$$V_6 \equiv 2[m] - [m^2], \tag{6f}$$

where,

$$[m^n] \equiv \ln\left|\frac{\partial\langle m^n\rangle}{\partial T}\right|. \tag{7}$$

In critical phenomena the thermodynamic quantities are expected to behave in the vicinity of the phase transition as[19,24,25]

$$c_v \sim t^{-\alpha}, \tag{8}$$

$$\chi \sim t^{-\gamma}, \tag{9}$$

$$m \sim t^{\beta}, \tag{10}$$

$$\xi \sim t^{-\nu}, \tag{11}$$

where $t=|T-T_c|/T_c$ is the reduced temperature, m is the magnetization, ξ is the correlation length, and α, β, γ, and ν are critical exponents. Although the critical temperature depends on the details of the system in consideration, it is observed that the critical exponents are to some extent universal depending only on a few fundamental factors.[19,24,25] The systems are thus divided in a small number of universality classes. Systems belonging to the same universality class share the same critical exponents. Critical exponents depend only on the spatial dimensionality of the system, the symmetry and dimensionality of the order parameter, and the range of the interactions within the system.

In a finite system as those used in Monte Carlo simulations the divergences in the thermodynamic quantities are replaced by smooth functions. Finite-size effects are therefore of great importance in the analysis of the results of Monte Carlo simulations. The theory of finite-size scaling[19,25] provides one way to extract information concerning the thermodynamic limit properties from results obtained in finite systems. The basic assumption of this theory is that in the vicinity of the phase transition the finite-size effects should depend on the ratio between the linear dimension of the system (L) and the correlation length (ξ). According to such theory, the specific heat, susceptibility, and magnetization for a finite system in the vicinity of the phase transition behave as

$$c_v \approx c_\infty(t) + L^{\alpha/\nu}\mathcal{C}(tL^{1/\nu}), \tag{12a}$$

$$\chi \approx L^{\gamma/\nu}\mathcal{X}(tL^{1/\nu}), \tag{12b}$$

$$m \approx L^{-\beta/\nu}\mathcal{M}(tL^{1/\nu}), \tag{12c}$$

where $\mathcal{M}$, $\mathcal{X}$, and $\mathcal{C}$ are proper derivatives of the free energy. At T_c ($t=0$) these functions are constants and the size dependence of specific heat, susceptibility, and magnetization follows a pure power law. The size dependence of the pseudocritical temperature $[T_c(L)]$ is[19,25]

$$T_c(L) = T_c + wL^{-1/\nu}, \tag{13}$$

where T_c is the critical temperature in the thermodynamic limit. Using the size dependence of the magnetization [Eq. (12)] and the definition of the moments of the magnetization in Eq. (6), one can easily show that such functions behave as

$$V_j \approx (1/\nu)\ln L + \mathcal{V}_j(tL^{1/\nu}), \tag{14}$$

for $j=1,2,\ldots,6$. At $t=0$ the functions $\mathcal{V}_j(tL^{1/\nu})$ are constants and then the curves for all V_j have the same slope,[23] thus providing a very precise method to determine the critical exponent ν and the critical temperature.

Concerning the fourth-order Binder's cumulant it is expected that for large enough lattice sizes, the curves for $U_4(T)$ should cross at the same point $U^*=U(T=T_c)$. Besides that, its size dependence is expected to be[26]

$$U_4 \approx \mathcal{U}_4(tL^{1/\nu}). \tag{15}$$

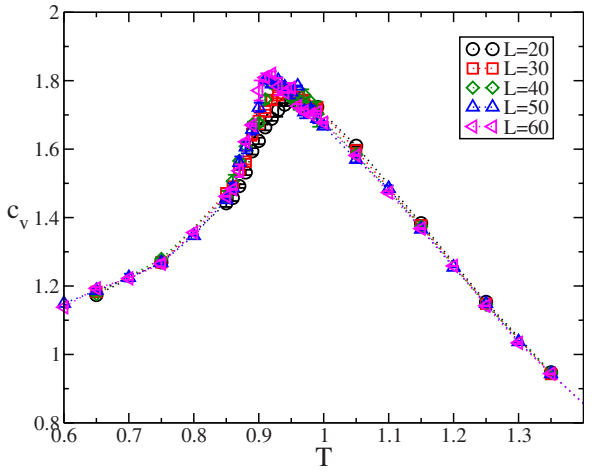

FIG. 3. (Color online) Specific heat as a function of temperature for $20<L<60$. Note that it displays small size effects.

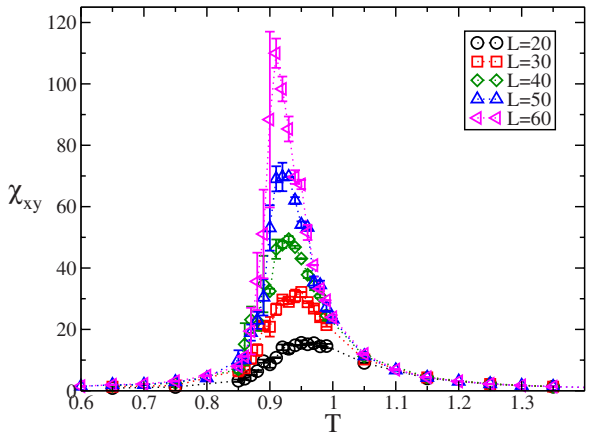

FIG. 4. (Color online) Planar susceptibility as a function of temperature for $20<L<60$.

III. RESULTS

Our results were obtained as follows. A preliminary set of simulations was carried out for lattices of sizes $L=20$, 30, 40, 50, and 60 averaging over 10^5 configurations for temperatures between 0.6 and 1.35. At each temperature the first $100\times L^2$ MCS were discarded in order to drive the system to thermal equilibrium. The results for the planar magnetization, specific heat, planar susceptibility, and Binder's cumulant are shown in Figs. 2–5, respectively. Once we estimated the position of the specific heat and of the planar susceptibility peaks, $T_m^c(L)$ and $T_m^\chi(L)$, another set of simulations was carried out using the histogram reweighting techniques[19,21,22] for $20\leq L\leq 120$. The histogram temperatures were chosen at the maxima of the susceptibilities and specific heat for each L. At least three simulations using independent random number sequences were used to build the histograms up. Each histogram consists of at least 2×10^7 configurations. For some lattices sizes we also did simulations at slightly different temperatures for using the multiple-histogram techniques[22] to put the error bars inside satisfactory levels.

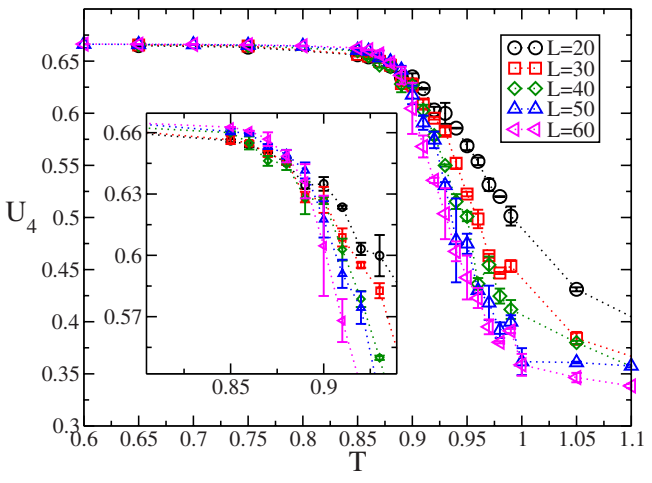

FIG. 5. (Color online) Fourth-order Binder's cumulant of planar magnetization as a function of temperature. The inset shows a zoom in the crossing region.

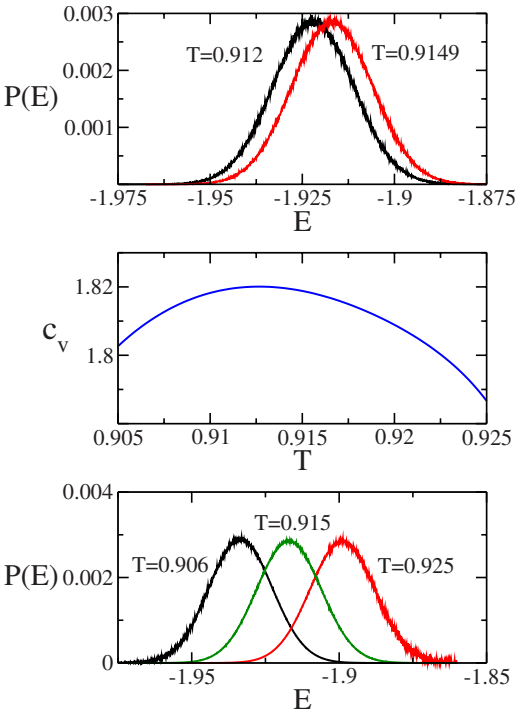

FIG. 6. (Color online) Top: Normalized histograms obtained in two simulations performed at $T=0.912$ and $T=0.9149$. In each simulation 10^7 configurations were used to build these histograms up. Middle: Specific heat calculated by using the multiple-histogram technique. Bottom: Probability distribution of energy at $T=0.906$, $T=0.915$, and $T=0.925$ obtained by using the multiple-histogram technique.

We exemplify the use of the histograms in Fig. 6. The top figure shows the normalized histograms, $P(E)$, obtained in two simulations at temperatures close to the maxima of the specific heat for $L=80$. Using the multiple-histogram technique[22] we calculated the specific heat shown in the middle picture of the same figure. At the bottom we show the energy probability distribution $P(E)$ obtained by using the multiple histograms at three different temperatures. In Fig. 7 we show a log-log plot of the maximum value of the planar susceptibility (χ_{xy}^m) as a function of the lattice size for L

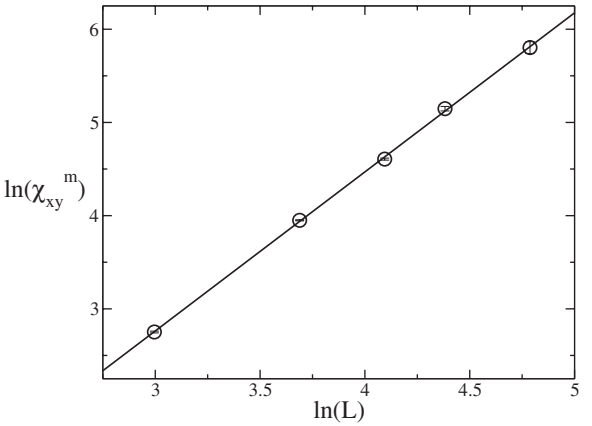

FIG. 7. Log-log plot of size dependence of planar susceptibility at $T_c(L)$. The solid line is the best fit with $\gamma/\nu=1.71(2)$.

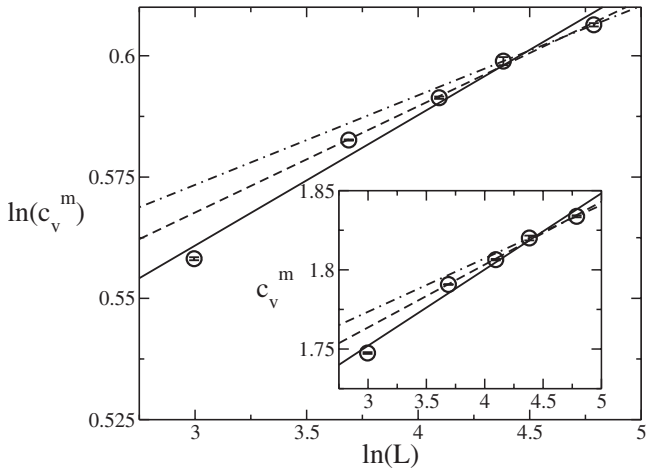

FIG. 8. Log-log plot of the size dependence of the specific heat at $T_c(L)$. The solid line is the best fit using all points while the dashed line is the best fit excluding the smallest lattice size ($L=20$) and the dotted-dashed line is the best fit using only $L=80$ and $L=120$. The inset shows c_v^m versus $\ln(L)$. The symbols and lines are the same as in the outer plot. Note that the slope of the curves diminishes as we exclude smaller lattice. The error bars are shown inside the symbols.

$=20$, 40, 60, 80, and 120. From finite-size scaling we expect that $\chi_{xy}^m \propto L^{\gamma/\nu}$ [see Eq. (12)]. Note that as expected the plot of $\ln(\chi_{xy}^m) \times \ln(L)$ is well adjusted by a straight line giving the exponent $\gamma/\nu=1.71(2)$. In critical phenomena it is expected that the specific heat diverges as a power law or logarithmically as in the Ising universality class. In Fig. 8 we show a log-log plot of the maximum value of the specific heat as a function of the lattice size. The inset shows the same results in a semilogarithmic plot. Note that a pure power-law scenario or a logarithmic divergence does not adjust the data points for the entire lattice sizes range. Besides that, as the small lattice sizes are excluded from the adjusted data points the slope diminishes (see Fig. 8), which indicates a nondivergent specific heat. This scenario will be explored in more details in Sec. IV. Using the crossing points of the fourth-

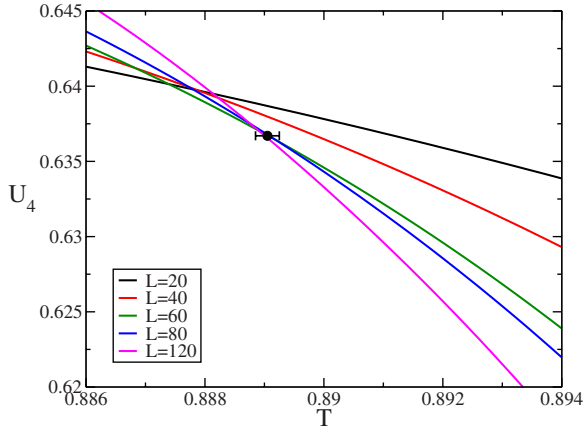

FIG. 9. (Color online) Fourth-order Binder's cumulant obtained using the multiple-histogram techniques. The point represents the estimated critical temperature using the crossing point for the largest lattices. Error bars are not shown for clarity.

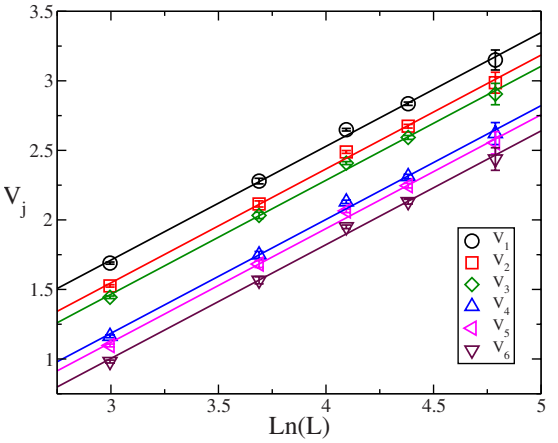

FIG. 10. (Color online) Size dependence of the six moments V_j at $T=0.8928$. It is expected at the critical temperature all quantities to have the same slope $1/\nu$.

order Binder's cumulant of Fig. 5 as a first estimate for the critical temperature T_c, another set of simulations was carried out at temperatures closer to that one for $20 \leq L \leq 120$. Multiple histograms were built up using up to 4×10^7 configurations. In Fig. 9 we show the crossing region of the Binder's cumulant obtained in this new set of simulations. We used the crossing point of the largest lattices sizes to estimate the critical temperature [$T_c^{U_4}=0.889(2)$]. Using the six moments of the magnetization defined in Eq. (6) we obtained another estimate for the critical temperature. The moments were also used to obtain an estimate of the exponent ν. In Fig. 10 we show V_j [see Eq. (6)] as a function of $\ln(L)$ at $T=0.8928$. Note that all quantities have almost the same slope. In Fig. 11 we show the values of $1/\nu$ obtained by using a linear fit of V_j as a function of $\ln(L)$ for temperatures close to $T=0.893$ for each j. Using this method we estimate the critical temperature $T_c^{V_j}=0.893(1)$ and the exponent $\nu=1.22(9)$. Using this value for ν we plotted in Fig. 12 the pseudocritical temperatures $T_c^{c_v}(L)$ (temperature at which the maximum of the specific heat occurs for the lattice of size L) and $T_c^{\chi}(L)$

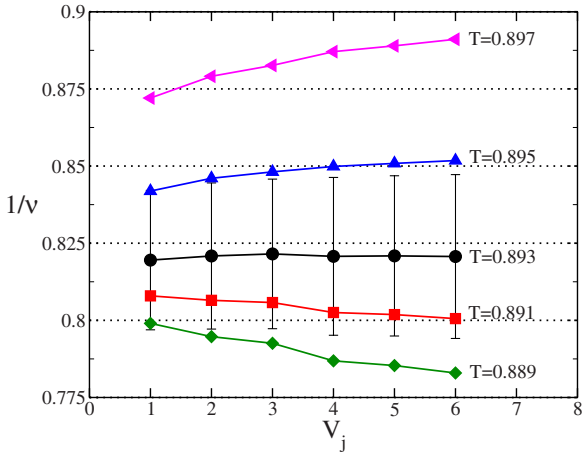

FIG. 11. (Color online) Value of $1/\nu$ obtained by linear fits of V_j versus $\ln(L)$ for each value of j at different temperatures. Note that for $T \approx 0.893$ the value of $1/\nu$ is almost the same for all quantities. In this figure only the error bars for $T=0.893$ are shown for clarity.

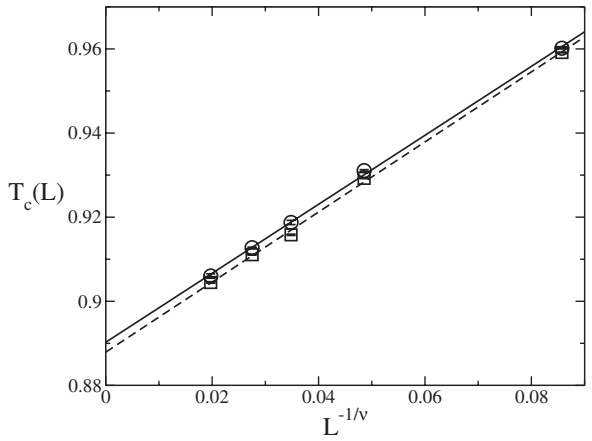

FIG. 12. Pseudocritical temperatures as a function of $L^{-1/\nu}$ for $1/\nu=0.82$. Circles are $T_c^{c_v}(L)$ and squares are $T_c^{\chi}(L)$. The solid and dashed lines are the best linear fits of $T_c^{c_v}(L)$ and $T_c^{\chi}(L)$, respectively. The intercepts are $T_c^{c_v}=0.890(3)$ and $T_c^{\chi}=0.888(2)$ for the specific heat and susceptibility, respectively.

(temperature at the maximum of the planar susceptibility) as a function of $L^{-1/\nu}$. Note that as expected the data in Fig. 12 are well adjusted by a straight line. Using Eq. (13) two other estimates for the critical temperatures, $T_c^{c_v}=0.890(3)$ and $T_c^{\chi}=0.888(2)$, were obtained. Our best value for the critical temperature is thus the mean value of the previous estimates $T_c^{U_4}$, $T_c^{V_j}$, $T_c^{c_v}$, and T_c^{χ}. It gives $T_c=0.890(4)$. Plotting $\ln(M_{xy})$ versus $\ln(L)$ at T_c (see Fig. 13) it is possible to obtain the exponent β/ν. From a linear adjust we get $\beta/\nu=0.15(4)$.

In summary, we obtained the mean critical temperature $T_c=0.890(4)$ and the critical exponents $\nu=1.22(9)$, $\gamma=2.1(2)$, and $\beta=0.18(5)$. Using these values we can check their validity by using the scaling functions of Eq. (12). In Figs. 14–16 we show the scaling plots of the planar magnetization, planar susceptibility, and fourth-order Binder's cumulant [see Eqs. (12) and (15)]. Note that in all cases we have a very good collapse of the curves for different lattice sizes.

IV. DISCUSSION AND CONCLUSIONS

We performed extensive Monte Carlo simulations to study the planar-to-paramagnetic phase transition in the d-AH

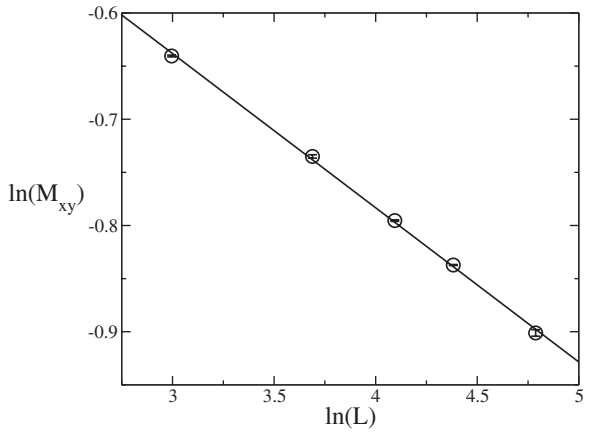

FIG. 13. $\ln(M_{xy})$ versus $\ln(L)$ at $T=T_c$. The solid line is the best fit and the slope is $\beta/\nu=0.15(4)$.

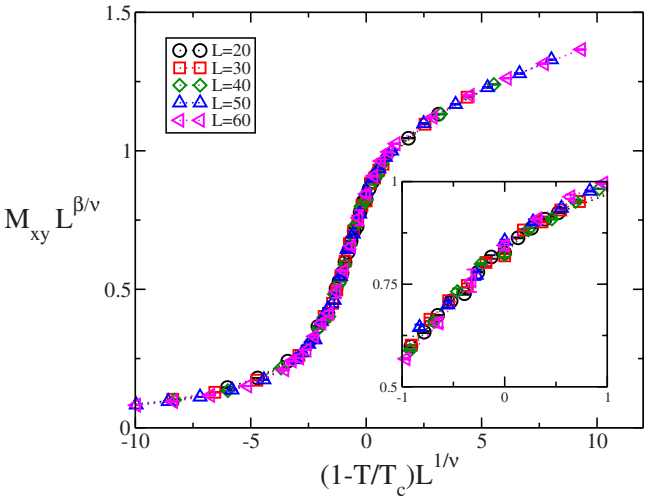

FIG. 14. (Color online) Scaling plot of magnetization using $T_c=0.890$, $1/\nu=0.82$ and $\beta/\nu=0.15$ [see Eq. (12)]. The inset shows a zoom near $T=T_c$. Note that the curves for different lattice sizes collapse into a single curve.

model in a bilayer system. Using the size dependence of the magnetization moments, planar susceptibility, planar magnetization, fourth-order Binder's cumulant, and specific heat, we obtained the critical temperature $T_c=0.890(4)$ and the critical exponents $\nu=1.22(9)$, $\gamma=2.1(2)$, and $\beta=0.18(5)$. The scaling plots of the magnetization, susceptibility, and fourth-order Binder's cumulant are shown in Figs. 14–16, respectively. A very good collapse of the curves for different lattice sizes is obtained for all quantities. This is a strong evidence of the validity of those values.

As can be seen in Fig. 8 a pure power law or logarithmic divergence cannot describe our specific-heat data for the entire lattice sizes range (note the size of the error bars in Fig. 8). As the smaller lattice sizes are discarded the slope of the curve for $\ln(c_v^m)$ versus $\ln(L)$ diminishes indicating a nondivergent specific heat. This hypothesis is corroborated by the

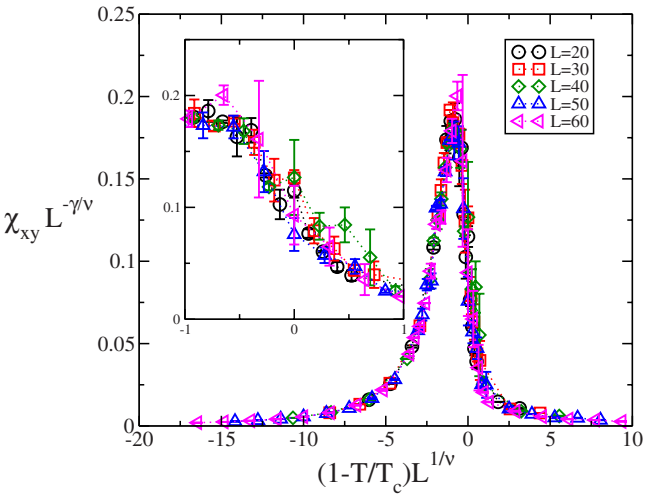

FIG. 15. (Color online) Scaling plot of susceptibility using $T_c=0.890$, $1/\nu=0.82$ and $\gamma/\nu=1.71$ [see Eq. (12)]. The inset shows a zoom near $T=T_c$. Note that the curves for different lattice sizes collapse into a single curve.

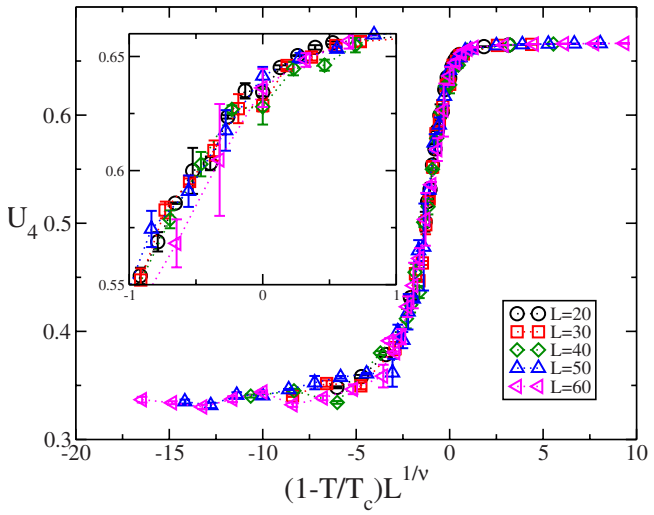

FIG. 16. (Color online) Scaling plot of fourth-order Binder's cumulant using $T_c=0.890$ and $1/\nu=0.82$ [see Eq. (15)]. The inset shows a zoom near $T=T_c$. Note that the curves for different lattice sizes collapse into a single curve.

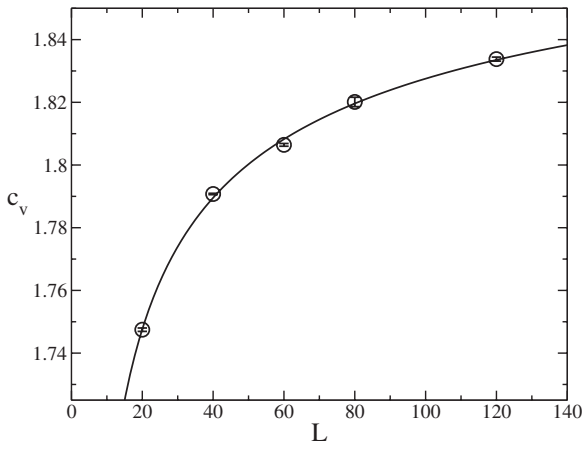

FIG. 17. Nonlinear least-squares fit of c_v^m according to $c_v^m=c_\infty+b/\ln(L)+aL^{-0.33}$. If we use the values of a, b, and c_∞, obtained in this fit and perform another fit adjusting α/ν, a, b, and c_∞, we observe that the new value of α/ν is -0.325 and the difference in χ^2 is negligible.

scaling laws. Using the exponents ν, γ, and β that we obtained and the scaling law[19,25] $\alpha+2\beta+\gamma=2$ or $\nu d=2-\alpha$, we get $\alpha\approx-0.4$. A negative value for the exponent α indicates that the specific heat does not diverge in the thermodynamic limit. Nevertheless, it does not exclude the possibility of the presence of a finite maximum at T_c. The observed behavior of the specific heat resembles that of a BKT phase transition where the specific heat does not diverge but presents a finite maximum close to T_{BKT}.[27] In the BKT phase transition it is observed that the specific heat presents a maximum close to the critical temperature and as the lattice size L increases the height of the specific-heat maximum also increases approaching an asymptotic value c_∞ as $L\to\infty$. This behavior is very similar to that obtained in this work. The results of Maier and Schwabl[18] for the planar-to-paramagnetic phase transition in the dipolar XY model also predict a nondivergent specific heat. In order to make our data consistent with a negative value of the exponent α we *conjecture* the existence of a correction to the scaling function. This correction must be an additive analytical term to be included in the scaling function of the specific heat. Our ansatz is a term such as $c_v^m\approx c_\infty+b/\ln(L)+aL^{\alpha/\nu}$. For $\alpha/\nu<0$, c_v^m increases up to the maximum value c_∞ for $L\to\infty$. In Fig. 17 we show the best fit using the above function where the value of α/ν was fixed to -0.33 as obtained by using our results and scaling laws. It is worthy to note that in order to confirm this conjecture analytical results and simulations in larger systems are needed, but these are beyond the scope of this paper.

Concerning the presence of long-range order in this system some remarks are in order. First, note that the finite-size scaling theory used here is based on a critical phenomenon where at low temperatures the order parameter is nonzero in the thermodynamic limit, i.e., this theory implicitly assumes the presence of long-range order.[19,25] The finite-size scaling functions of Eq. (12) describe our data with good accuracy for the entire temperature range employed in our simulations. We can thus conclude that since the theory for systems presenting long-range order can describe our results for the entire temperature range, our system should present long-range order. It is notable that the exponents we obtained do not match those of well-known universality classes. Especially the exponent $\nu=1.22>1$ is quite unusual. This could be an *indication* that the planar-to-paramagnetic phase transition in the d-AH model belongs to another universality class characterized by a nondivergent specific heat and by the exponents $\nu=1.22(9)$, $\gamma=2.1(2)$, and $\beta=0.18(5)$.

In a recent paper Rapini *et al.*[14] also studied the same model (d-AH) in a square lattice using a cutoff at $r_0=5a$. Their results are consistent with a BKT phase transition. Nevertheless, our results for the two-layer system is fully consistent with an order-disorder phase transition as discussed above. One can then conjecture that the inclusion of the second layer in the system may reinforce the transition, exposing its actual character. It may be that the consideration of the entire range of dipole interaction could have a similar effect. However, this is a *speculation*. This hypothesis cannot be confirmed without a very detailed study of systems with true long-range dipolar interactions. Indeed, if this is the case one could expect obtaining similar results to those of Maier and Schwabl[18] for the dipolar XY model. Nevertheless, the exponents we obtained are clearly distinct from those of Maier and Schwabl and the finite value of ν that we found is a clear indication of an algebraic divergent correlation length instead of an exponential divergence as they found. Moreover, the finite-size scaling theory used is based in a power-law divergence of the correlation length [see Eq. (11)]. On the other hand, Bander and Mills[28] showed by using renormalization group arguments that for the Heisenberg model, without dipolar interactions, the existence of an infinitesimal easy-axis anisotropy is sufficient to bring the system to the Ising universality class. In this way the observed order-disorder behavior can be a consequence of the easy-axis anisotropy. Another point that must be raised is that the intrinsic anisotropic character of dipolar interactions can be

responsible for the observed behavior instead of the long-range character (a similar behavior was observed recently in Ref. 29). In short, much work has still to be done in order to fully understand the planar-to-paramagnetic phase transition in ferromagnetic thin films where dipolar interactions are important.

ACKNOWLEDGMENTS

We would like to thank D. P. Landau for helpful discussions. Numerical calculation was done in the Linux cluster at Laboratório de Simulação at Departamento de Física–UFMG. We are grateful to CNPq and Fapemig (Brazilian agencies) for financial support.

*lucasmol@fisica.ufmg.br
†bvc@fisica.ufmg.br

[1] R. P. Cowburn, D. K. Koltsov, A. O. Adeyeye, M. E. Welland, and D. M. Tricker, Phys. Rev. Lett. **83**, 1042 (1999).
[2] W. A. Moura-Melo, A. R. Pereira, R. L. Silva, and N. M. Oliveira-Neto, J. Appl. Phys. **103**, 124306 (2008).
[3] S. A. Leonel, I. A. Marques, P. Z. Coura, and B. V. Costa, J. Appl. Phys. **102**, 104311 (2007).
[4] D. P. Pappas, K.-P. Kämper, and H. Hopster, Phys. Rev. Lett. **64**, 3179 (1990).
[5] R. Allenspach and A. Bischof, Phys. Rev. Lett. **69**, 3385 (1992).
[6] N. D. Mermin and H. Wagner, Phys. Rev. Lett. **17**, 1133 (1966).
[7] J. M. Kosterlitz and D. J. Thouless, J. Phys. C **6**, 1181 (1973).
[8] V. L. Berezinskii, Sov. Phys. JETP **32**, 493 (1971).
[9] S. V. Maleev, Sov. Phys. JETP **43**, 1240 (1976).
[10] P. Bruno, Phys. Rev. B **43**, 6015 (1991).
[11] K. De'Bell, A. B. MacIsaac, and J. P. Whitehead, Rev. Mod. Phys. **72**, 225 (2000).
[12] C. Santamaria and H. T. Diep, J. Magn. Magn. Mater. **212**, 23 (2000).
[13] M. Carubelli, O. V. Billoni, S. A. Pighín, S. A. Cannas, D. A. Stariolo, and F. A. Tamarit, Phys. Rev. B **77**, 134417 (2008).
[14] M. Rapini, R. A. Dias, and B. V. Costa, Phys. Rev. B **75**, 014425 (2007).
[15] M. Rapini, R. A. Dias, D. P. Landau, and B. V. Costa, Braz. J. Phys. **36**, 672 (2006).
[16] A. B. MacIsaac, K. De'Bell, and J. P. Whitehead, Phys. Rev. Lett. **80**, 616 (1998).
[17] J. P. Whitehead, A. B. MacIsaac, and K. De'Bell, Phys. Rev. B **77**, 174415 (2008).
[18] P. G. Maier and F. Schwabl, Phys. Rev. B **70**, 134430 (2004).
[19] D. P. Landau and K. Binder, *A Guide to Monte Carlo Simulations in Statistical Physics* (Cambridge University Press, New York, 2005).
[20] J. M. Thijssen, *Computational Physics* (Cambridge University Press, New York, 1999).
[21] A. M. Ferrenberg, in *Computer Simulation Studies in Condensed Matter Physics*, edited by D. Landau, K. Mon, and H. Schüttler (Spring-Verlag, Berlin, 1991), Vol. 3.
[22] A. M. Ferrenberg and R. H. Swendsen, Phys. Rev. Lett. **63**, 1195 (1989).
[23] K. Chen, A. M. Ferrenberg, and D. P. Landau, Phys. Rev. B **48**, 3249 (1993).
[24] H. E. Stanley, *Introduction to Phase Transition and Critical Phenomena* (Clarendon, Oxford, 1971).
[25] *Finite Size Scaling and Numerical Simulation of Statistical Systems*, edited by V. Privman (World Scientific, Singapore, 1990).
[26] K. Binder, Phys. Rev. Lett. **47**, 693 (1981).
[27] A. Cuccoli, V. Tognetti, and R. Vaia, Phys. Rev. B **52**, 10221 (1995).
[28] M. Bander and D. L. Mills, Phys. Rev. B **38**, 12015 (1988).
[29] J. F. Fernández and J. J. Alonso, Phys. Rev. B **76**, 014403 (2007).